Am J Physiol Endocrinol Metab 311: E367–E379, 2016.
First published June 14, 2016; doi:10.1152/ajpendo.00077.2016.

The expansion of adult stem/progenitor cells and their marker expression fluctuations are linked with pituitary plastic adaptation during gestation and lactancy

Alicia Maldré Vaca,[1] Carolina Beatriz Guido,[1] Liliana del Valle Sosa,[1] Juan Pablo Nicola,[2] Jorge Mukdsi,[1] Juan Pablo Petiti,[1] and Alicia Ines Torres[1]

[1]*Centro de Microscopía Electrónica, Instituto de Investigaciones en Ciencias de la Salud-Consejo Nacional de Investigaciones Científicas y Técnicas (CONICET), Facultad de Ciencias Médicas, Universidad Nacional de Córdoba, Haya de la Torre Esq. Enrique Barros, Ciudad Universitaria, Córdoba, Argentina; and* [2]*Centro de Investigaciones en Bioquímica Clínica e Inmunología, Centro de Investigaciones en Bioquímica Clínica e Inmunología-CONICET, Facultad de Ciencias Químicas, Universidad Nacional de Córdoba, Haya de la Torre y Medina Allende, Ciudad Universitaria, Córdoba, Argentina*

Submitted 29 February 2016; accepted in final form 10 June 2016

Vaca AM, Guido CB, Sosa LD, Nicola JP, Mukdsi J, Petiti JP, Torres AI. The expansion of adult stem/progenitor cells and their marker expression fluctuations are linked with pituitary plastic adaptation during gestation and lactancy. *Am J Physiol Endocrinol Metab* 311: E367–E379, 2016. First published June 14, 2016; doi:10.1152/ajpendo.00077.2016.—Extensive evidence has revealed variations in the number of hormone-producing cells in the pituitary gland, which occur under physiological conditions such as gestation and lactancy. It has been proposed that new hormone-producing cells differentiate from stem cells. However, exactly how and when this takes place is not clear. In this work, we used immunoelectron microscopy to identify adult pituitary stem/progenitor cells (SC/P) localized in the marginal zone (MZ), and additionally, we detected GFRa2-, Sox2-, and Sox9-positive cells in the adenoparenchyma (AP) by fluorescence microscopy. Then, we evaluated fluctuations of SC/P mRNA and protein level markers in MZ and AP during gestation and lactancy. An upregulation in stemness markers was shown at term of gestation (AT) in MZ, whereas there were more progenitor cell markers in the middle of gestation and active lactancy. Concerning committed cell markers, we detected a rise in AP at beginning of lactancy (d1L). We performed a BrdU uptake analysis in MZ and AP cells. The highest level of BrdU uptake was observed in MZ AT cells, whereas in AP this was detected in d1L, followed by a decrease in both the MZ and AP. Finally, we detected double immunostaining for BrdU-GFRa2 in MZ AT cells and BrdU-Sox9 in the AP d1L cells. Taken together, we hypothesize that the expansion of the SC/P niche took place mainly in MZ from pituitary rats in AT and d1L. These results suggest that the SC niche actively participates in pituitary plasticity during these reproductive states, contributing to the origin of hormone cell populations.

pituitary gland; stem cell/progenitor markers; marginal zone; gestation; lactancy

THE PITUITARY GLAND IS A CENTRAL REGULATOR of growth, reproduction, and endocrine physiology and functions by relaying signals from the hypothalamus to various target organs. Its major endocrine function resides in the pars distalis (PD), which contains five different specialized hormone-producing cell types whose proportions can alter under different physiological conditions (31), such as the reproductive cycle (23), gestation, and lactancy (22, 47). This hormone output must be fine-tuned and adapt swiftly to changing needs, thereby requiring dynamic and accurate functional and quantitative remodeling of the hormonal cells (36, 45). It has been described that the generation of new endocrine cells occurs in different ways, including the mitosis of already differentiated cells (10, 37), transdifferentiation between distinct cell phenotypes (40, 50), and differentiation of stem/progenitor cells (8). All three processes combine their effects in dynamic cell adaptations, but a single mechanism may predominate depending on the particular physiological situation. The plasticity of the pituitary gland is in fact one of the most important features that allows the existence of stem cells (SC) to be postulated in this adult endocrine tissue (39).

The development of the pituitary gland begins with a structure called Rathke's pouch, which invaginates from the oral ectoderm and grows out around the remaining lumen-denominated cleft. Embryonic progenitor cells appear to reside in the marginal zone (MZ) around the cleft. Indeed, cells in this zone markedly proliferate and ostensibly migrate to the emergent PD, where they develop further into different hormonal cell lineages (27). During postnatal life, multilayered and heterogeneous MZ cells, referred to as the niche for putative pituitary SC, are able to retain some features of their embryonic nature (49).

The SC have been reported in different adult organs on the basis of their capacity to proliferate and carry out self-renewal, a differentiation potential, and the ability to regenerate tissue after cell loss and are able to express key marker genes (32, 35, 41), with the principal ones being the transcription factors Oct-4 and Sox2, which are involved in the maintenance of pluripotency in the genome of SC (48, 55). The Sox9 progenitor marker, a member of the SoxE subfamily, is important in embryonic and postnatal development (9) and participates in differentiation programs by activation of tissue-specific genes (26). In the pituitary gland, it has been postulated that the transcription factor Prop1 might play a role as a trigger in the terminal differentiation process of progenitor cells, leading to the development of endocrine cells (53, 54). Prop1 positively regulates the expression of the pituitary-specific transcription factor Pit-1, with this factor being critical for normal thyrotroph, somatotroph, and lactotroph development. Furthermore, Prop1 and Pit-1 have been associated with the maturation of committed cell lineages (28, 44).

Address for reprint requests and other correspondence: A. I. Torres, Centro de Microscopía Electrónica, INICSA-CONICET, Facultad de Ciencias Médicas, Universidad Nacional de Córdoba, Haya de la Torre esq. Enrique Barros, Ciudad Universitaria, CP 5000, Córdoba, Argentina (e-mail: atorres@cmefcm.uncor.edu).

Several nonendocrine cells have been described as being SC and proposed to maintain pituitary homeostasis by the generation of new endocrine cells. Nevertheless, the identity and functional position of adult pituitary SC and their role in the pituitary plasticity described in physiological conditions are not well understood. Numerous studies have been able to demonstrate that these nonendocrine cells in the adult pituitary gland express stemness markers; for example, a side population that efficiently excludes the Hoechst 33342 vital dye has been shown to generate sphere-forming cells (8). Also, pituitary colony-forming cells that display a notable clonal potential have been isolated (30). However, the only common marker studied for these cells was Sca1, and to date its position in the pituitary is not well established. The presence of Sox2+ and Sox9+ cells in the MZ and clusters scattering in the adenoparenchyma (AP) have allowed these transcription factors to be proposed as markers of pituitary SC/progenitors (SC/P) or transit-amplifying cells (15, 58). In addition, a niche of putative SC/P in the pituitary expresses the Glial cell line-derived neurotropic factor receptor-α2 (GFRa2), with this specific marker proposed for pituitary SC being localized in MZ cells (19) and recently detected in scarce AP cells (18).

Extensive evidence has revealed significant changes in the number of different PD cell populations in certain defined physiological conditions to meet the endocrine demands of the organism (3), with an increased mitotic activity of lactotrophs being reported during the reproductive cycle and lactancy (2, 38). However, exactly how and when this takes place is not clear. It has been proposed that during plastic adaptations and basic cell turnover, new hormone-producing cells differentiate from nonendocrine cells, which represent SC (36). Therefore, gestation and lactancy represent an adequate physiological model to test cell differentiation of potential SC. In an attempt to elucidate this mechanism, we identified the SC/P in the pituitary gland by fluorescence and electron microscopy and evaluated the possible changes in SC/P-associated markers expressed in the MZ and the adenoparenchyma during gestation and lactancy. Furthermore, the specific contribution of these cells in the maintenance of pituitary homeostasis in response to physiological hormonal requirements was also analyzed.

MATERIALS AND METHODS

Animals and experimental design. Virgin female Wistar rats aged 10–12 wk were examined by vaginal smear cytology and assigned to the estrous or diestrous II phases. Only rats that completed the estrous phases over two cycles were included in this study. Rats were mated with proven fertile males and then divided in the following groups: *group A* [gestation (G)], i.e., copula (COP), rats in the estrous phase that had sperm in their vaginal smear at 5 days of gestation after copula (d5G), at 15 days after copula (d15G), and at term of gestation (AT); and *group B* [lactancy (L)], i.e., pregnant rats that were transferred to individual cages until the day of parturition. At birth, the number of litters was adjusted to eight pups, and then the mothers were euthanized at the beginning of lactancy (d1L or early lactancy) or after 4 days of lactancy (d4L or active lactancy).

All rats were bred and housed at the Animal Research Facility of the INICSA-CONICET-School of Medicine, National University of Córdoba, under controlled temperature (21 ± 3°C) and lighting conditions (14:10-h light-dark cycle), having free access to commercial rodent food and tap water. Animals were kept in accordance with the National Institutes of Health *Guide for the Care and Use of Laboratory Animals* (1996), and the experiments were approved by the Institutional Animal Care Committee of School of Medicine, National University of Córdoba.

Characterization of cells in the MZ by high-resolution light microscopy, transmission electron microscopy, and ultrastructural immunocytochemistry. MZ cells were studied in three hemipituitaries from each experimental group after being fixed by immersion in 4% (vol/vol) glutaraldehyde and 4% (wt/vol) formaldehyde in 0.1 M cacodylate buffer, treated with 1% osmium tetroxide (Sigma, St. Louis, MO), dehydrated, and embedded in Araldite (Electron Microscopy, Hatfield, PA). For high-resolution light microscopy analysis, semithin (200 μm) sections were stained with blue toluidine, and MZ cells were observed. The MZ cell ultrastructures were analyzed in thin sections (60 μm), stained with uranyl acetate/lead citrate, and examined in a Zeiss-Leo 906-E electron microscope.

For ultrastructural immunocytochemistry (UICC), the animals of each group were euthanized by decapitation, and pituitary glands were removed and cut into two small pieces in coronal orientation. Then, these glands were fixed for 4 h in 4% (wt/vol) formaldehyde with 0.75% (vol/vol) glutaraldehyde in 0.1 M cacodylate buffer. The fixed tissues were dehydrated by a series of increasing concentrations of ethanol and immersed in LR White (Electron Microscopy) before being embedded in gelatin capsules to avoid contact of the resin with oxygen. The ultrathin sections were cut and placed on nickel grids. The method of UICC used was described previously (12). Briefly, sections were incubated with blocking solution composed of the three proteins, 5% bovine serum albumin (BSA), 5% goat normal serum, and 1% cold fish skin gelatin, and then reacted with anti-vimentin (mouse 1:100 Novocastra), anti-GFRa2 (rabbit, 1:100; Santa Cruz Biotechnology, Dallas, TX), anti-Sox2 (rabbit, 1:50; Millipore, Billerica, MA), anti-Sox9 (mouse, 1:100; Santa Cruz Biotechnology), or anti-Oct-4 (rabbit, 1/50; Santa Cruz Biotechnology) as the primary antiserum. Then, they were exposed to goat anti-mouse or anti-rabbit IgG labeled with a 15-nm gold complex (1:30; Electron Microscopy). The grids were stained with uranyl acetate (Sigma) and examined using a Zeiss LEO 906-E electron microscope. To validate the specificity of the immunostaining, we performed a negative control, replacing the primary antiserum with 1% BSA in PBS followed by the secondary antibody.

Ultrastructural morphometric analysis was performed on electron micrographs obtained from coronal sections of two different MZ areas separated from each other by 50 μm in all of the experimental groups. To avoid duplicate counting of the same cell, only one large section from each block was mounted on a 200-mesh nickel grid. Then, 100 electron micrographs were taken randomly from each section at a magnification of ×16,700, covering 100–200 cells/animal. Using ImageJ 1.47v (Wayne Rasband; National Institutes of Health), we counted all gold particles in the cytoplasm and the nucleus compartment per area unit, named labeling density (11). The number of gold particles was referenced to 10 μm^2 of cytoplasm or nucleus compartment.

BrdU uptake in AP and MZ cells. 5-Bromo-2′-deoxiuridina (BrdU; Sigma), which is incorporated in DNA instead of thymidine in cells in the S phase of the cell cycle, was dissolved in phosphate-buffered saline (PBS; 50 mg/ml) and injected intraperitoneally at a dose of 50 μg/g rat weight 12 h before decapitation.

Four pituitary glands per experimental group were fixed in 4% buffered formaldehyde, dehydrated, and embedded in paraffin. These pituitaries were then cut, deparaffined, rehydrated, and washed in 0.1 M PBS before being treated with 3% H_2O_2 for 15 min to inhibit endogenous peroxidase activity, after which 5% PBS-BSA was applied for 30 min to block nonspecific binding of the secondary antibody. Pituitary sections were incubated overnight in a 1:100 solution containing anti-BrdU (GE Healthcare Life Sciences), and then the slides were washed with PBS and exposed to a biotin-labeled secondary antibody against mouse IgG at room temperature for 30 min and to ABC complex for 30 min (Vector Laboratories, Burlin-

game, CA). Subsequently, the slides were immersed in a solution containing 3-3′-diaminobenzidine (Sigma) in 0.1 M Tris buffer, pH 7.2, containing 0.03% H_2O_2 before being counterstained with hematoxylin, dehydrated, and cover-slipped with mounting liquid (Sigma). Negative controls were also performed by applying the same protocol, but BrdU antibody was omitted.

Three different levels from the coronal pituitary sections, including MZ and AP, which were separated from each other by 50 μm, were sampled per rat and used for morphometric analysis. All results were pooled for each individual animal. Immunoreactive cells were observed using a light microscope at a magnification of ×400, with the number of BrdU -mmunoreactive cells being counted from two MZ layers and from a total of 5,000 AP cells obtained from random samples taken from each rat.

Immunodetection of SC/P markers and BrdU incorporation in frozen pituitary gland samples. The pituitary gland of the different experimental groups studied were placed in Crioplast (Biopack, Buenos Aires, Argentina) and immersed in liquid nitrogen for a few minutes until the solidification of the embedding medium and stored at −80°C. For immunodetections, the cryostat sections were fixed in absolute methanol, incubated with PBS-BSA 5%, and then reacted with anti-GFRa2 (rabbit, 1:100; Santa Cruz Biotechnology), anti-Sox2 (mouse, 1:200; Millipore), anti-Sox9 (rabbit, 1:200; Santa Cruz Biotechnology), or anti-BrdU (mouse, 1:100; GE Bioscience Healthcare). Subsequently, the slides were exposed to a secondary antibody Alexa 594 anti-rabbit (1:1,000; Invitrogen, Carlsbad, CA) or anti-mouse Alexa 488 (1:1,000; Invitrogen, Eugene, OR) for 1 h at room temperature and mounted with fluoromount (Sigma) containing DAPI.

For double immunodetection, analysis was performed on consecutive days to avoid nonspecific immunolabeling given by the secondary antibody. Briefly, during the 1st day, samples were incubated with BrdU (mouse, 1:100), GFRa2 (rabbit, 1:100), Sox9 (rabbit, 1:200), or prolactin (PRL; rabbit 1:10,000; National Hormone and Pituitary Program, Torrance, CA) antibodies. Then they were washed with PBS and exposed to a secondary antibody labeled with Alexa 594 (1/1,000). On the 2nd day, the samples were washed with PBS and incubated with BrdU. Then they were reacted with secondary antibody Alexa 488 (1:1,000). To validate the specificity of the immunostaining, negative controls were performed by applying the same protocol but replacing primary antibody with 5% PBS-BSA.

Laser capture microdissection and RNA isolation. The pituitary glands of rats corresponding to the G and L groups were immersed in buffer solution with 0.1 M Tris, zinc salts (5 g of $ZnCl_2$, 6 g of $ZnAc_2.2\ H_2O$, and 0.1 g of $CaAc_2$), and 30% sucrose and then frozen in tissue-freezing medium (Crioplast; Biopack, Buenos Aires, Argentina). These samples were cut into 15-μm sections using a cryostat (Shandon Cryotome SME), transferred to polyethylene naphthalate membrane, fixed in 70% ethanol at −20°C, and dehydrated on activated silica. MZ and AP regions were morphologically identified and captured using laser dissection microscopy (Leica LDM6000). Dissected areas were collected, and the total RNA was isolated using an illustra RNAspin Mini RNA Isolation Kit (GE Healthcare Life Sciences), following the manufacturer's recommendations.

Complementary DNA synthesis was performed by incubating 11 μl of total RNA extracted from MZ and AP regions with 9 μl of reverse-transcription reaction mixture containing 4 μl of FS buffer (5×), 1 μl of dNTPs (10 mM), 1 μl of random hexamers (50–250 ng), 1 μl of M-MLV reverse transcriptase (200 U/μl), 0.5 μl of RNase out (40 U/μl), and 1.5 μl of DTT (0.1 M). Reverse-transcription reaction was performed on a 5332 Eppendorf Mastercycler using the following temperature cycle: 10 min at 70°C, 1 min on ice, 10 min at 25°C, 1 h at 37°C, and 15 min at 70°C.

Gene expression analysis by quantitative PCR. Real-time PCR analysis was performed on an ABI Prism 7500 detection system (Applied Biosystems, Foster City, CA) using Power SYBR Green PCR Master Mix (Applied Biosystems, Thermo Fisher Scientific, Waltham, MA). The gene-specific primer sets are described in Table 1. Relative changes in gene expression were calculated using the $2^{-\Delta\Delta C_T}$ method normalized against the housekeeping gene β-actin. For each pair of primers, a dissociation plot resulted in a single peak, indicating that only one cDNA species was amplified. Amplification efficiency for each pair of primers was calculated using standard curves generated by serial dilutions of cDNA obtained from embryos at 10 wk of gestation. All primers were from GBT Oligos Genbiotech (Buenos Aires, Argentina).

Statistical analysis. Statistical analysis was carried out using an analysis of variance with the Tukey posttest (SPSS Statistics for Windows, version 17.0). The results are given as means ± SE, and the data were obtained from three replicates measured for three independent experiments. The significance level chosen was $P < 0.05$.

RESULTS

Characterization and topographic localization of the SC niche in the MZ. First, we attempted to localize topographically the MZ and study the morphology of the cells sited in this area by high-resolution light and electron microscopy. The MZ is composed of two layers of cells (Fig. 1), with one of these outlining the cleft and the other situated below in tight contact. The cells that composed the first layer of the MZ had in general a cuboid appearance with an increased nucleus/cytoplasm relationship and an absence of secretory granules in the cytoplasm. Some of these cells possessed apical extensions such as cilia and microvilli, which are hallmarks associated with the SC phenotype, and the cells that presented microvilli and cilia

Table 1. *Oligonucleotide primers and expected amplicon sizes for qPCR amplification of the markers analyzed*

Marker	Nucleotide Sequence	Genebank Accession No. (Position of Amplified Fragment)
Oct-4	Forward: 5′-ACACCTGGCTTCAGCTTCG-3′ Reverse: 5′-CAGAGTCTCCACGCCAACTT-3′	NM_001009178 (89–448)
Sox2	Forward:5′-CTCTGTGGTCAAGTCCGAGG-3′ Reverse: 5′-CTCTTTTGCACCCCTCCCAA-3′	NM_001109181 (1,092–1,379)
Sox9	Forward: 5′-TGAAGATGACCGACGAGCAG-3′ Reverse: 5′-GTGTGGCTTGTTCTTGCTGG-3′	XM_003750950 (406–676)
GFRa2	Forward: 5′-TCAGGGACTTCACGGAAAAC-3′ Reverse: 5′-AGATGTGCAGGTGGTGATGA-3′	NM_012750 (1,136–1,332)
Prop1	Forward: 5′-AGTCAGCCTTTGGGAGGAAC-3′ Reverse: 5′-TAGTGACCGCTCTTGCTTCC-3′	NM_153627 (248–368)
Pit-1	Forward:5′-GGAGAGCACAGCAAACCTTC-3′ Reverse: 5′-ATGGCTACCACAGGCAAGTC-3′	L01506 (748–980)
B-actina	Forward: 5′-ACCCACACTGTGCCCATCTA-3′ Reverse: 5′-CGGAACCGCTCATTGCC-3′	NM_031144 (556–845)

qPCR, quantitative PCR; GFRa2, glial cell line-derived neurotropic factor receptor-α2.

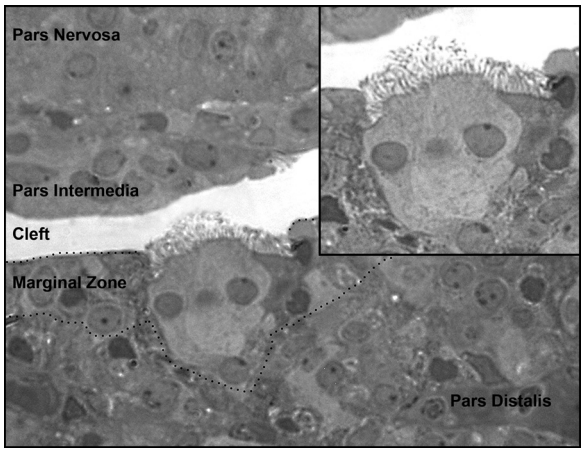

Fig. 1. Topographic localization of the marginal zone (MZ) in the adult pituitary gland. The gland has 3 regions: the pars distalis (PD) containing the epithelial endocrine cells and the MZ (indicated by the dotted line) outlining the cleft that comprises the 1st and 2nd layers of cells from the PD, the pars nervosa (PN) comprising axon terminals and supportive pituicytes, and the pars intermedia (PI) containing melanocortin cells. *Inset* shows in detail the apical extensions of a cell located in the MZ. Original magnification, ×400; *inset*, ×1,000.

in the apical membrane were oriented toward the cleft (Fig. 2). The second MZ layer is composed of cells with similar morphological characteristics described for SC and others with a fusiform shape similar to supporting cells referred to as mesenchymal cells (MC).

To characterize completely the SC niche, we identified a marker of supporting MC such as vimentin by UICC. Vimentin expression was observed in MZ cells, being dispersed in the cytoplasm and unassociated with the organelles. These vimentin-positive cells were arranged below the first line MZ cells (Fig. 3, *A* and *B*).

Subcellular localization of markers associated with the SC/P phenotype. Subcellular localization and the distribution of markers associated with the SC/P phenotype at the MZ of adult pituitaries were analyzed by UICC. The expression of Oct-4 and GFRa2 was intense in cells localized at the region around the cleft, which then decreased toward the adenohypophysis. In particular, the GFRa2 expression was dispersed in the cytoplasm of cells localized in the first layer of the MZ (Fig. 4*A*), with Oct-4 being observed in the nucleus and cytoplasm of these cells (Fig. 4*B*). In addition, both SC markers were observed in cells with apical membrane differentiations. The expression of Sox2 and Sox9 was observed in the first line of MZ cells and also in cells with morphological SC characteristics that composed the second MZ line. An interesting observation was that Sox2 had a remarkable immumoreactivity within the nucleus of MZ cells. Meanwhile, Sox9 immunogold labeling was weaker in the nucleus and cytoplasm of cells localized in this zone (Fig. 4, *C* and *D*).

In parallel, we performed assays using immunofluorescence microscopy to search for and identify GFRa2-, Sox2-, or Sox9-positive cells in the adult pituitary gland. As shown in Fig. 4, *E* and *F*, we observed GFRa2- and Sox2-positive cells, respectively, in the AP as a few sparse cells, whereas Sox9-positive cells were observed to be scattered in AP and are displayed in Fig. 4*G*.

Analysis of mRNA levels of SC/P and committed cell markers in the MZ and adenoparenchyma during gestation and lactancy. To assess whether the stemness, progenitor markers, and gene expression associated with committed cells exhibited any changes in the MZ and AP during the reproductive states under study, we used laser capture microdissection to individually isolate each zone. Total RNA was isolated and the mRNA expression of marker genes evaluated by real-time PCR.

Gene expression in the MZ. The mRNA levels of the SC markers GFRa2, Sox2, and Oct-4 exhibited the highest expression at the end of gestation (AT) compared with their expression at earlier gestation stages. Moreover, we observed a significant decrease in the expression of these markers during lactancy (Fig. 5*A1*). The progenitor gen marker Sox9 displayed

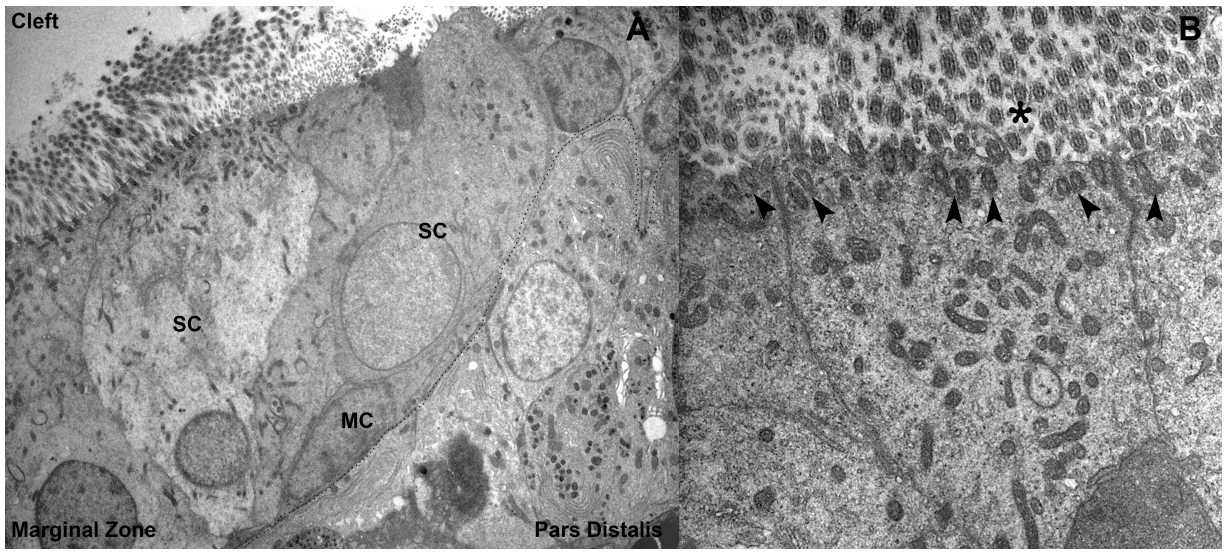

Fig. 2. The MZ in the adult pituitary gland. *A*: electron micrograph of a pituitary gland section from an adult rat reveals the fine structure of cells located in the MZ (indicated by the dotted line). Some MZ cells of the 1st layer identified as stem cells (SC) have apical extensions such as cilia and microvilli. Below this layer there are some cells having a fusiform shape, with this morphology being compatible with mesenchymal cells (MC). Original magnification, ×2,100. *B*: representative micrograph of typical ultrastructural characteristics of cilia. Arrowheads indicate basal bodies. *Axonema. Original magnification, ×6,000.

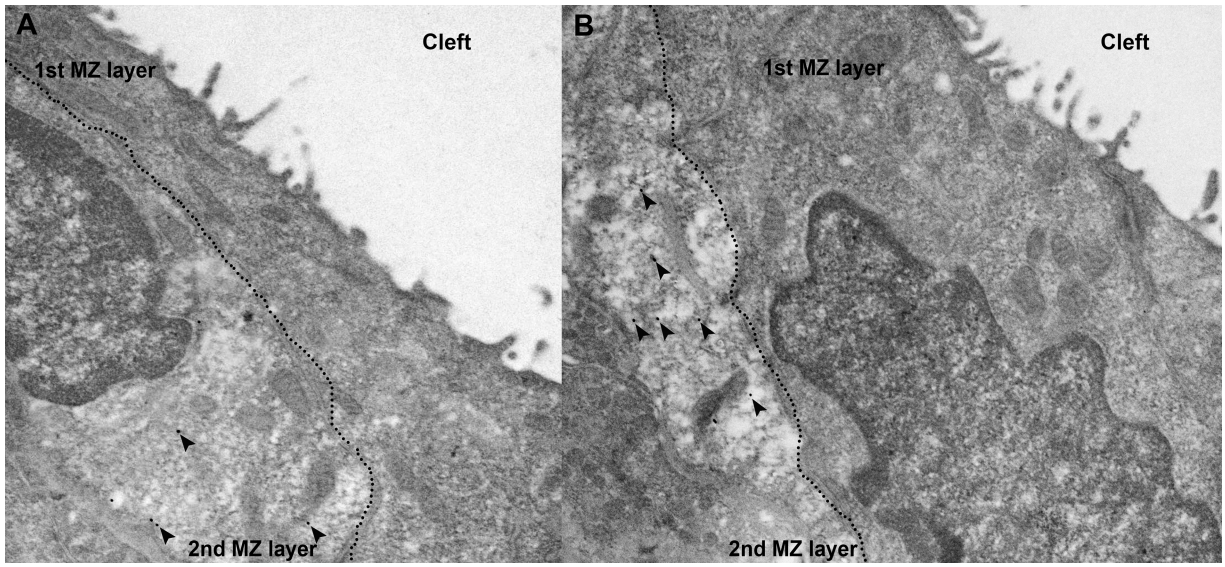

Fig. 3. The ultrastructural localization of MC was examined in pituitary glands of adult rats by vimentin ultrastructural immunocytochemistry. *A*: representative micrograph of a vimentin-positive cell localized in the 2nd layer of the MZ below a cell with apical extensions. *B*: cytoplasm observed in the 2nd MZ layer is an extension of the cell exhibited in *A*, showing vimentin-positive expression. Dotted line indicates the limit between the 1st and the 2nd layer of MZ. Original magnification, ×16,700.

a different expression pattern during the reproductive stages, showing a twofold increase at d15G before returning to basal levels at term of gestation but exhibiting a significant increase at 4 days of active lactancy (Fig. 5*A2*). The expression of the lineage-committed markers Prop1 and Pit-1 did not exhibit any significant variations during gestation. Nevertheless, we observed a significant increase in the expression levels of Prop1 and Pit-1 at AT and early lactancy compared with their expression during gestation (Fig. 5*A3*).

Gene expression in the adenoparenchyma. The GFRa2, Oct-4, and Sox2 mRNA levels showed a significant reduction at d5G and d15G with respect to COP, although Oct-4 mRNA exhibited an increase at AT. The lactancy stimuli induced a striking rise in GFRa2 mRNA levels but a significant reduction in the Sox2 and Oct-4 mRNA levels (Fig. 5*B1*). Conversely, Sox9 mRNA levels did not show significant variations during gestation and lactancy stages (Fig. 5*B2*).

For the period of gestation, the mRNA levels of the lineage-committed marker Prop1 did not show a significant modification. Meanwhile, Pit-1 mRNA expression showed a significant increase at d15G and AT. In addition, at early lactancy, Prop1 and Pit-1 mRNA displayed a significant increase. However, after 4 days of lactancy, Prop1 mRNA levels decrease and Pit-1 return to AT levels (Fig. 5*B3*). In addition, we analyzed the relationship between Pit-1/Prop1 in MZ vs. AP. In MZ, Prop1 expression was greater than Pit-1 in AT (0.69 ± 0.085) and d1L (0.70 ± 0.058), whereas this relation was inverted ($P < 0.05$) in AP of the same groups (AT: 1.81 ± 0.14; d1L: 1.70 ± 0.23).

Expression of SC/P markers in MZ cells during gestation and lactancy. To evaluate the expression of the SC/P markers GFRa2, Oct-4, Sox2, and Sox9 in MZ cells throughout different reproductive states such as gestation and lactancy, we quantified the immunogold labeling using an electron microscope. This technique is a reliable tool and allowed us to quantify the markers of SC/P cells localized specifically in MZ and to determine their possible fluctuations in response to changes in hormonal surges during physiological conditions.

GFRa2. GFRa2 expression in the cytoplasm of MZ cells quantified by morphometric analysis was similar at COP and d5G. However, there was a marked reduction in the middle of the gestation (d15G) compared with COP ($P < 0.05$) but a noticeable increase at term of gestation. At the beginning of lactancy, the GFRa2 expression revealed a significant decrease ($P < 0.05$ vs. AT), with this level maintained after 4 days of lactancy (Fig. 6*A*).

Oct-4 and Sox2. The Oct-4 expression quantified in the cytoplasmic compartment of the MZ cells was similar at COP and gestation (d5G, d15G). In contrast, the immunolabeled nuclear Oct-4 exhibited a significant decrease in the middle of gestation and at AT. During active lactancy (d4L), the nuclear and cytoplasmic Oct-4 expression showed a great increase compared with at AT ($P < 0.01$), but no significant differences between nuclear and cytoplasmic compartments were observed at COP, gestation, or early lactancy. However, in d4L, the immunolabeled Oct-4 revealed a different subcellular distribution, as a higher expression in the cytoplasm than in the nuclear compartment was observed (Fig. 6*B*).

The Sox2 expression exhibited a different subcellular distribution pattern, displaying higher levels in the nuclear compared with the cytoplasmic compartment at COP and d15G (COP CC vs. NC, $P < 0.05$, and d15G CC vs. NC, $P < 0.01$). During active lactancy, the expression of this marker in both subcellular compartments showed remarkable increases (d4L vs. AT, $P < 0.01$; Fig. 6C).

Sox9. The Sox9 expression was analyzed in both the nuclear and cytoplasmic compartments of cells localized in MZ during the gestation and lactancy groups. The morphometric study showed a significant decrease in Sox9 immunolabeled within the cytoplasmic compartment during gestation at d5G and d15G compared with at COP, with a noticeable dimi-

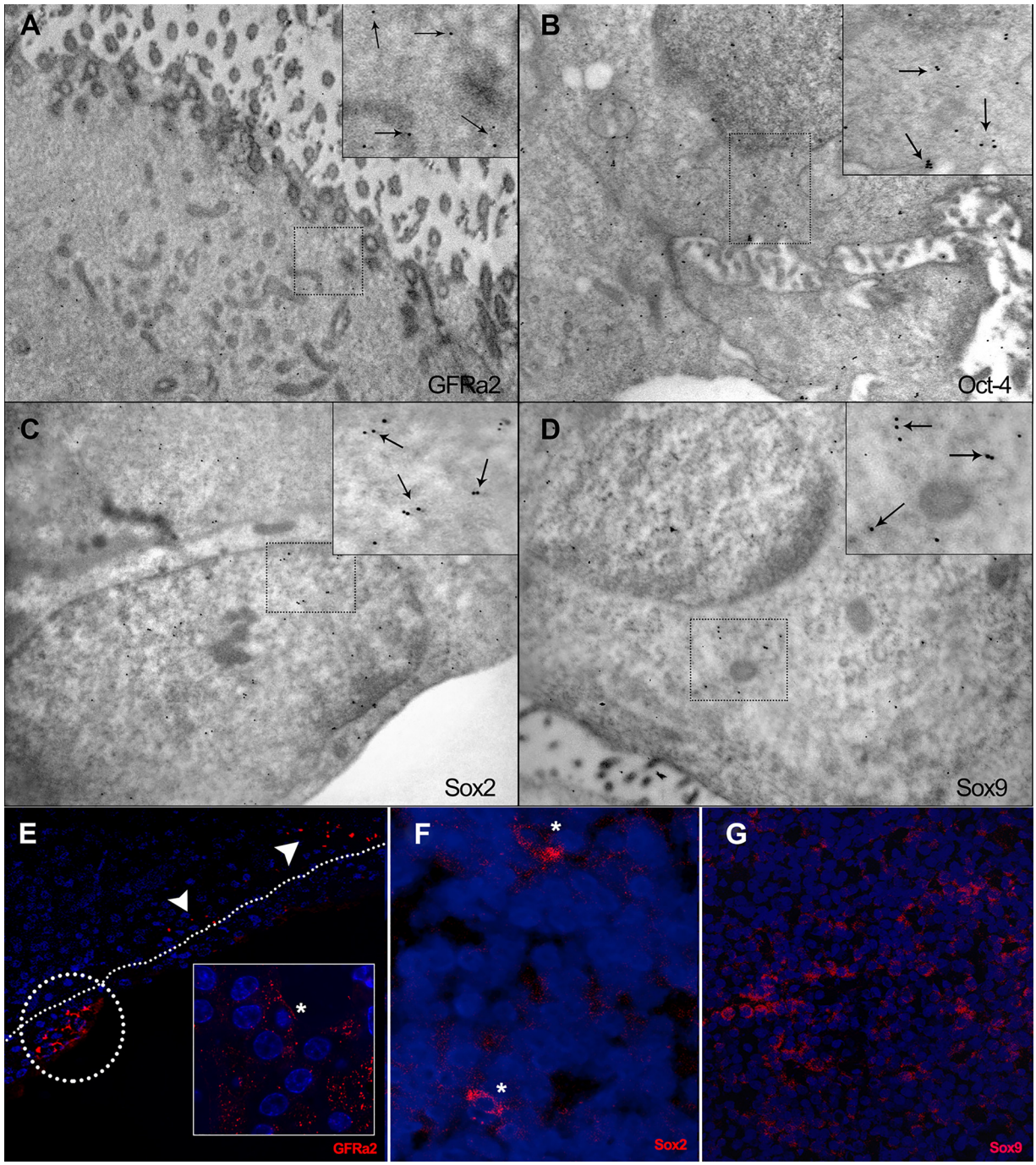

Fig. 4. Immunodetection of stem/progenitor cell (SC/P) markers in the MZ and adenoparenchyma (AP) of adult rat pituitary glands by electron and fluorescence microscopy. *A*: immunoelectron micrographs of Glial cell line-derived neurotropic factor (GDNF) receptor-α2 (GFRa2)+ cell localized in the 1st MZ layer displaying cilia at the apical membrane. Dotted square shows the location of the *inset* zone. The GFRa2+ cell exhibits moderate immunoreactivity in the cytoplasm near the plasma membrane. Original magnification, ×10,000. *B*: Oct-4+ cell identified by ultrastructural immunocytochemistry exhibiting microvilli in the apical membrane is situated in the 1st MZ layer. Immunogold labeling is intense at the cytoplasm. *C*: nucleus of the Sox2+ cell exhibits a stronger immunoreactivity than that observed in the cytoplasmic matrix using the colloidal gold technique. *D*: immunopositive MZ cell for Sox9 shows a free cytoplasmic labeling. Original magnification *B–D*, *insets*: ×16,700, with 15-nm gold particle identified by arrows. *E*: MZ cells (white dotted circle) and clusters cells in the adenoparenchyma exhibited the expression of the GFRa2 marker (white arrowheads). Dotted line indicates the MZ. Original magnification, ×200. *Inset*: *some cells of the MZ expressing the GFRa2 receptor on the surface. Original magnification, ×400. *F*: *scarce cells of the AP expressed Sox2 in the cytoplasm. Original magnification, ×400. *G*: scattered cells in the AP showed expression of Sox9. Original magnification, ×200.

nution also being observed in the d5G nuclear expression ($P < 0.05$ vs. COP) of this marker. However, this subcellular compartment displayed a significant increase at AT with respect to COP.

At early lactancy (d1L), the Sox9 expression determined in both subcellular compartments of MZ cells exhibited a remarkable increase compared with AT ($P < 0.01$ vs. AT) but decreased significantly after 4 days of active lactancy (Fig. 6*D*).

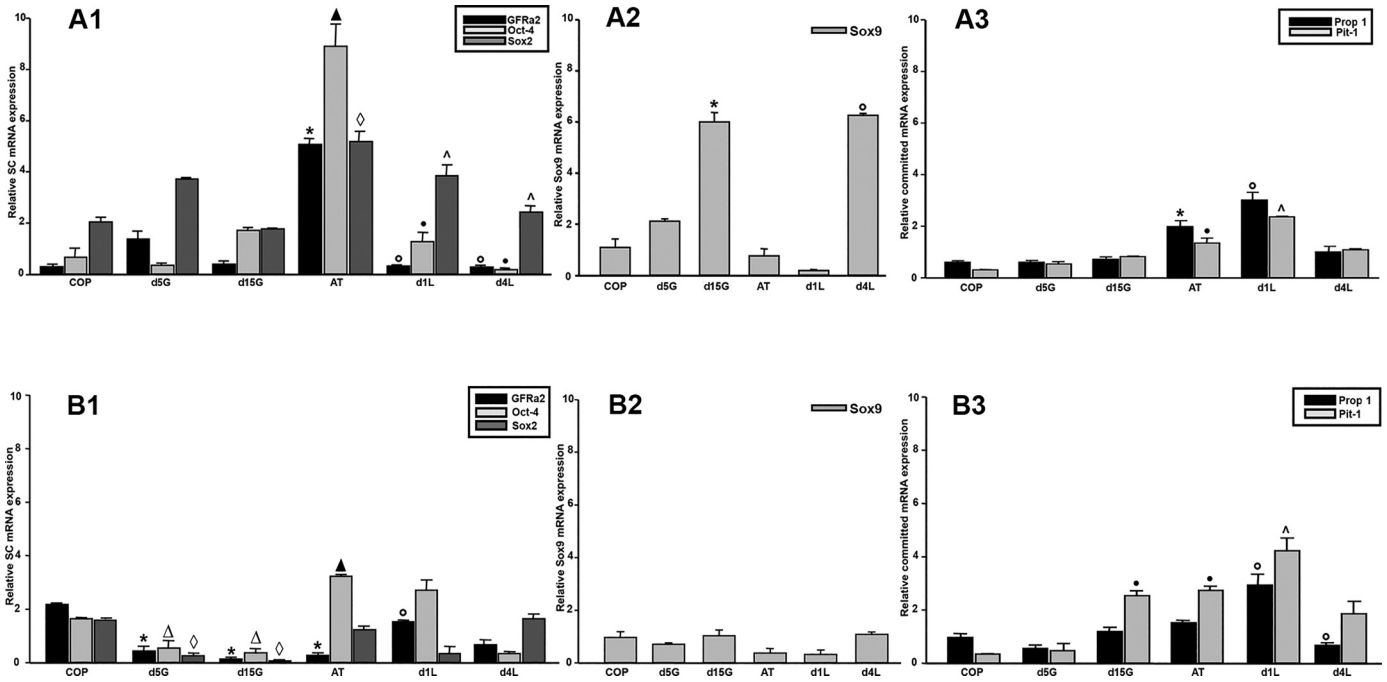

Fig. 5. Relative evaluation of SC/progenitor/committed mRNA levels in MZ and AP from gestation and lactancy pituitaries. *A1–A3*: GFRa2, Oct-4, Sox2, Sox9, Prop1, and Pit-1 mRNA levels quantified in MZ. *A1*: GFRa2 [*$P < 0.05$ AT vs. copula (COP)], Oct-4 (▲$P < 0.05$ AT vs. COP), and Sox2 (◇$P < 0.05$ AT vs. COP) show an increase at term of gestation but a decrease during lactancy [GFRa2: ○$P < 0.05$ beginning of lactancy (d1L) and 4 days of lactancy (d4L) vs. AT; Oct-4: ●$P < 0.05$ d1L and d4L vs. AT; Sox2: ^$P < 0.05$ d1L and d4L vs. AT]. *A2*: Sox9 increased at d15G and d4L (*$P < 0.05$ d15G vs. COP; ○$P < 0.05$ d4L vs. AT). *A3*: Prop1 and Pit-1 show the highest levels at AT and early lactancy (*$P < 0.05$ AT vs. COP; ○$P < 0.05$ d1L vs. COP). *B1–B3*: GFRa2, Oct-4, Sox2, Sox9, Prop1 and Pit-1 mRNA levels quantified in AP. *B1*: SC markers decrease during gestation (GFRa2: *$P < 0.05$, d5G, d15G, and AT vs. COP; Oct-4: △$P < 0.05$, d5G and d15G vs. COP; Sox2: ◇$P < 0.05$ d5G and d15G vs. COP). However, in AT rats, Oct-4 mRNA exhibits an increase with respect to at COP (▲$P < 0.05$, AT vs. COP). The GFRa2 shows the highest levels at d1L (○$P < 0.05$, d1L vs. AT), whereas Sox2 does not evidence any significant changes in all groups analyzed. *B2*: Sox9 progenitor marker does not exhibit any variations during gestation or lactancy. *B3*: Pit-1 levels show increase from the middle of gestation to early lactancy (●$P < 0.05$ d15G and AT vs. COP; ^$P < 0.05$ d1L vs. AT), whereas Prop1 exhibits an increase at d1L (○$P < 0.05$ d1L vs. AT). The mRNA expression was relatively quantified to that of β-actin. Results are shown as fold change of the mRNA levels for COP and AT groups. Data are representative of 3 independent experiments and were analyzed by ANOVA-Tukey test.

Cell proliferation in the MZ and adenoparenchyma during gestation and lactancy. To investigate a possible link between the SC/progenitor/committed marker variations and the MZ and AP cell proliferation during gestation and active lactancy, we analyzed the uptake of BrdU into the nucleus of these cells.

Marginal cell proliferation. The uptake of BrdU of MZ cells displayed a dynamic fluctuation during gestation and lactancy, with COP considered to be the starting point (4.48 ± 0.37%). At 5 and 15 days of gestation, we observed a twofold decrease in BrdU-positive MZ cells ($P < 0.01$ vs. COP), with the highest levels of MZ cell proliferation being recorded in the AT (10.15 ± 0.49%). The beginning of lactancy, d1L, revealed a significant reduction in BrdU-positive cells with respect to AT, which after 4 days of active lactancy had reached a fivefold decrease with respect to d1L (5.63 ± 0.21 and 1.06 ± 0.10%, respectively; Fig. 7*F*). Interestingly, more BrdU-immunopositive cells were observed in the first layer of MZ than in the second one (Fig. 7, *A–E*).

Adenoparenchyma cell proliferation. The number of BrdU-immunopositive AP cells was significantly higher at d5G than at COP (3.20 ± 0.05 and 2.29 ± 0.02%, respectively), with a significant decrease at term of gestation resulting in values similar to those at COP. In the early lactancy group, the proliferation of adenohypophysial cells showed a rise of 1.5-fold with respect to the values quantified at AT (3.59 ± 0.3 and 2.29 ± 0.09%, respectively), followed by a decrease of about eightfold at d4L (0.46 ± 0.07%) (Fig. 8, *A–F*).

Coimmunodetection of BrdU with GFRa2 or Sox9 expression. Finally, we carried out a double-immunofluorescence assay for BrdU uptake and GFRa2, a pituitary-specific SC marker that exhibited a high expression in the AT group, in which the BrdU incorporation peak was observed in the MZ. As shown in Fig. 9, *A* and *B*, the coimmunodetection for BrdU and GFRa2 in MZ cells was more evident in the AT group, attaining a twofold increase compared with the COP group (2.36 ± 0.72 and 0.29 ± 0.29%, respectively; Fig. 9*C*).

Bearing in mind that in the AP the highest cell proliferation values were observed in early lactancy and that Sox9 participated in the expansion of the progenitor cell population, we compared the percentage of BrdU- and Sox9-positive cells in AP vs. MZ (Fig. 9, *D* and *E*) and found that the number of BrdU-positive cells that expressed the Sox9 marker was significantly greater in the AP than the MZ in the d1L group (3.06 ± 0.43 vs. 1.22 ± 0.23%, respectively). In addition, we carried out a double-immunofluorescence assay for Sox9 and PRL, the main hormone expressed during lactancy. As shown in the Fig. 9*F*, only a few cells coexpressed Sox9 and PRL in the AP of the d1L.

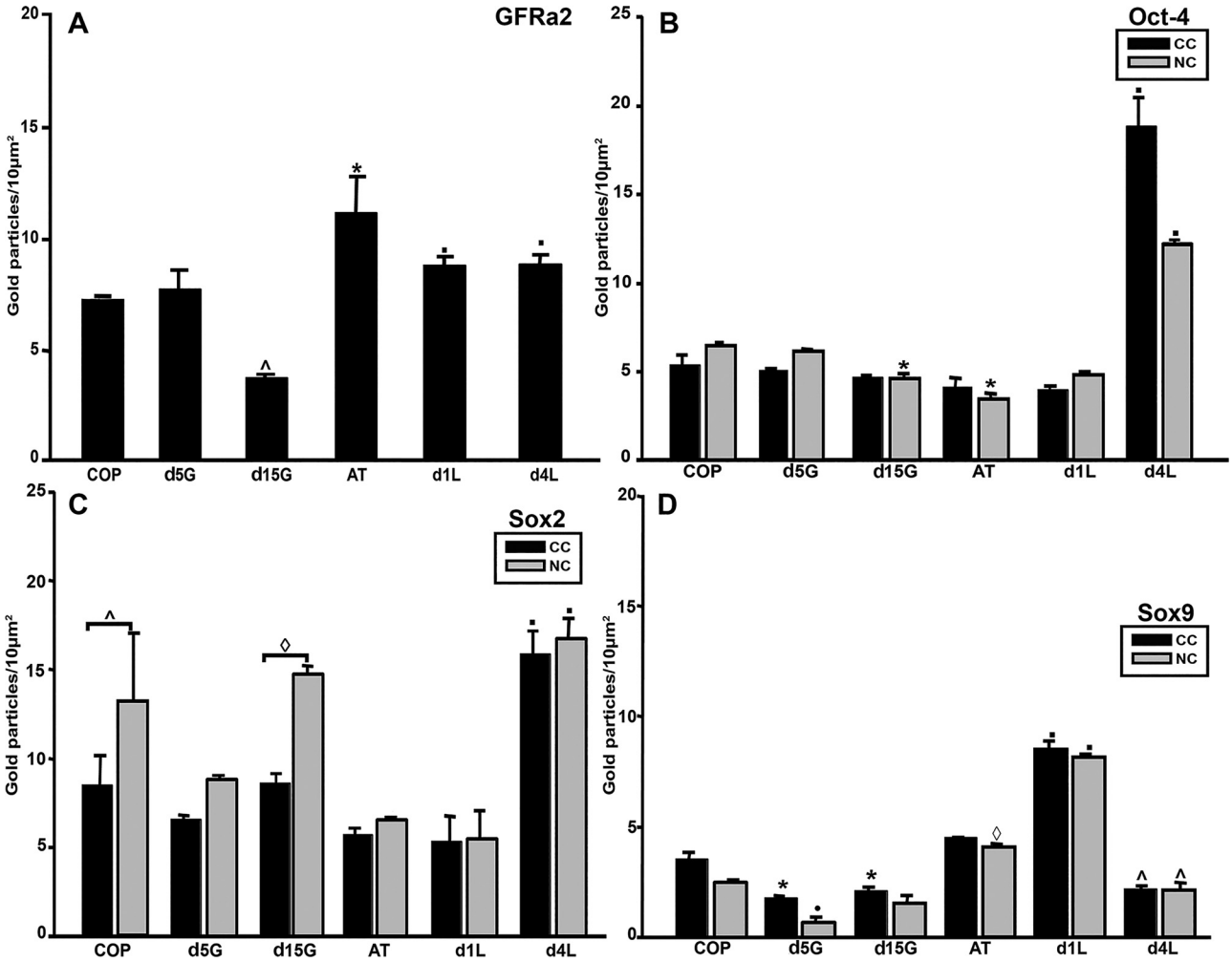

Fig. 6. Analysis of SC/P marker expression patterns in the cytoplasmic (CC) and nuclear (NC) compartments of the MZ cells. *A*: GFRa2 expression displays a remarkable increase at term of gestation. *$P < 0.05$, AT vs. COP; ^$P < 0.05$, d15G vs. COP; ■$P < 0.05$, d1L and d4L vs. AT. *B*: Oct-4 marker shows an increase in nuclear and cytoplasmic compartments in active lactancy. ■$P < 0.01$, d4L vs. AT; *$P < 0.01$, d15G and AT vs. COP (NC). *C*: a differential Sox2 distribution is exhibited between the nuclear and cytoplasmic compartments at COP (^$P < 0.05$, NC vs. CC) and d15G (◇$P < 0.01$ NC vs. CC), whereas in active lactancy Sox2 is increased in both subcellular compartments ■$P < 0.01$, d4L vs. AT. *D*: Sox9 marker expression displays an increase at early lactancy in both the nucleus and cytoplasm. ■$P < 0.01$, d1L vs. AT, with a notable decrease observed at d4L; □$P < 0.05$, d4L vs. AT; *$P < 0.05$, d5G and d15G vs. COP (CC); ■$P < 0.05$ d5G vs. COP and ◆P < 0.05 AT vs. COP (NC). Results are given as means ± SE from 3 independent experiments. The data were analyzed by the ANOVA-tukey test.

DISCUSSION

In the present study, we have demonstrated the participation of pituitary SC in the physiological cell turnover from fluctuations in SC/P mRNA and the protein level markers in combination with significant changes in the MZ cell proliferation rate, which took place during gestation and lactancy. Taking these findings into consideration, it appears that the SC pituitary niche actively participates in pituitary plasticity during these reproductive states, thereby being involved in the origin of mature hormone cell populations.

A stem cell niche is defined not only by the presence of tissue SC but also by the characterization of somatic support cells, which secrete essential factors for the maintenance of pluripotency in resident stem cells (51). An SC niche has been reported in the pituitary gland based on the detection of SC/P and mesenchymal cell markers in MZ by immunofluorescence (15, 19, 42). In the current investigation, we confirmed the presence of an adult pituitary SC niche and described for the first time through ultrastructural analyses the organization of MZ cells into two layers. GFRa2 and Oct-4 were expressed in the first layer of MZ cells, with some of these cells exhibiting microvillus and cilia in the apical membrane, thereby suggesting that they maintained the primary cilium as observed previously in the mitosis of embryonic cells that retained stem cell features (6). In both MZ layers, we identified Sox2- and Sox9-immunolabeled cells, whereas the vimentin-supporting cell marker (33) was visualized only in some cells of the second layer of this zone, which were precisely localized, surrounding the first layer of MZ cells. Moreover, in the AP of the adult pituitary gland, the GFRa2, Sox2, and Sox9 single positive cells and a few sparsely distributed groups were observed. In line with these results, it has been reported recently that scattered cells throughout the AP are positive for GFRa2 in the adult gland (18) in addition to some other previously identified SC markers such as Sox2, Sox9, and Klf4 (7, 20). These findings suggest the existence of multiple SC

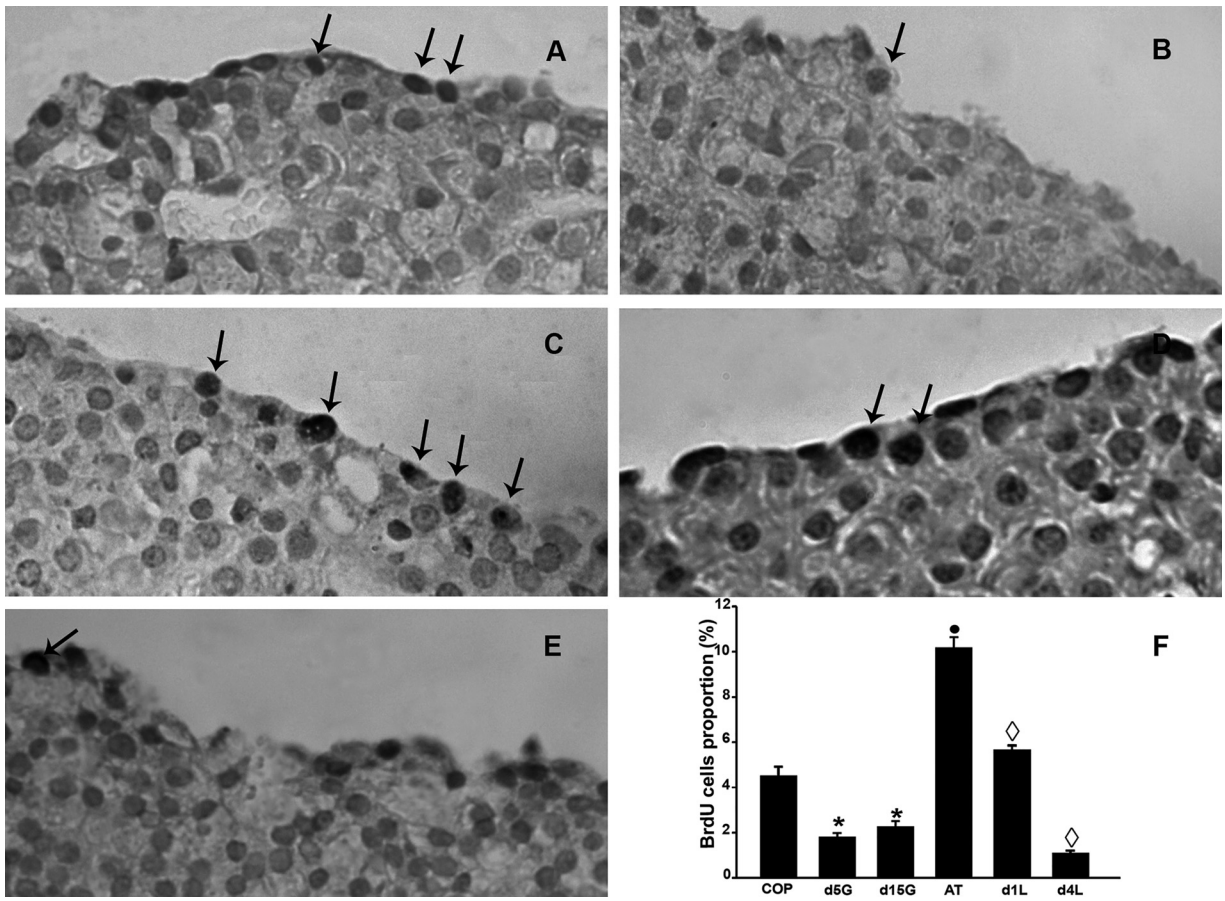

Fig. 7. Cell proliferation in MZ cells at gestation and lactation pituitaries. *A–E*: representative light microscope photomicrographs of BrdU-positive cells observed in rats at COP (*A*), d5G (representative of gestation; *B*), AT (*C*), d1L (*D*), and d4L (*E*). Arrows highlight selected cells that are positive for BrdU in the 1st and 2nd ZM layers. Original magnification, ×400. *F*: proportion of BrdU uptake in MZ cells. The BrdU incorporation peak occurs in AT pituitary gland in contrast with the other experimental groups. The d5G and d15G groups exhibit a decrease in BrdU (*$P < 0.01$, d5G and d15G vs. COP) but then a notable rise at AT (●$P < 0.01$, AT vs. COP), which is followed by a decrease during lactancy (◇$P < 0.01$, d1L and d4L vs. AT). The BrdU-positive nuclei staining is expressed as the percentage of the total nuclei counted from 2 MZ cell layers obtained for each rat. The data are shown as means ± SE of 4 animals/group, with data being analyzed using the ANOVA-Tukey test.

niches that could be favorable for dynamic and/or subtle cell adaptations.

A mitotic variability was described in the anterior pituitary of female rats (38, 56) in the estrous cycle and also during pregnancy and lactation (5, 13, 14), with estrogen being the principal cause for the increased lactotroph cell population (31). Considering the evidence of an SC/P niche in the adult pituitary and in an attempt to achieve a better understanding of the new endocrine cell supply during the cell turnover that occurs in states such as reproduction, we evaluated in vivo the SC/P contribution to the cell differentiation during gestation and lactancy. There is consistent evidence that GFRa2+ cells are located in the MZ of the adult pituitary (19), in agreement with our findings. However, little is known about their participation during new endocrine cell production. Our study revealed a noticeable increase in GFRa2 expression in the MZ at the end of gestation, suggesting its involvement in the SC recruitment that occurs in the MZ, thus giving rise to a progenitor cell population. Related to this, a recent report described that the upregulation of Ret receptor and its coreceptors GFRa1, GFRa2, and GFRa3 is key for hematopoietic SC survival and pluripotency and allows these cells to be distinguished from progenitor ones in the fetal liver (16). On the other hand, the greater mRNA GFRa2 expression in AP vs. MZ may have been related partly to the hormonal fluctuations that have been widely described in COP and lactation states, suggesting that the GFRa2+ AP cell groups may not represent isolated focal spots. Therefore, as described previously, the SC/P AP cell groups may be establishing a three-dimensional cooperating network throughout the gland, thereby allowing long-range communication between the stem cells, which would be important in coordinating their maintenance, proliferation, and differentiation activities (29, 34).

The other principal factors implicated in the maintenance of pluripotency in adult SC such as Oct-4 and Sox2 exhibited a notable increase in the mRNA levels in the MZ from the AT pituitary group. In addition, their protein expression levels showed an important rise in the active lactancy group (d4L). This dissociation observed between transcription and translation has also been reported for these markers in other studies performed at the early stages of the embryonic stem cell differentiation process, indicating that translational and posttranslational regulatory mechanisms have important roles in SC fate decisions and may reflect the nature of a

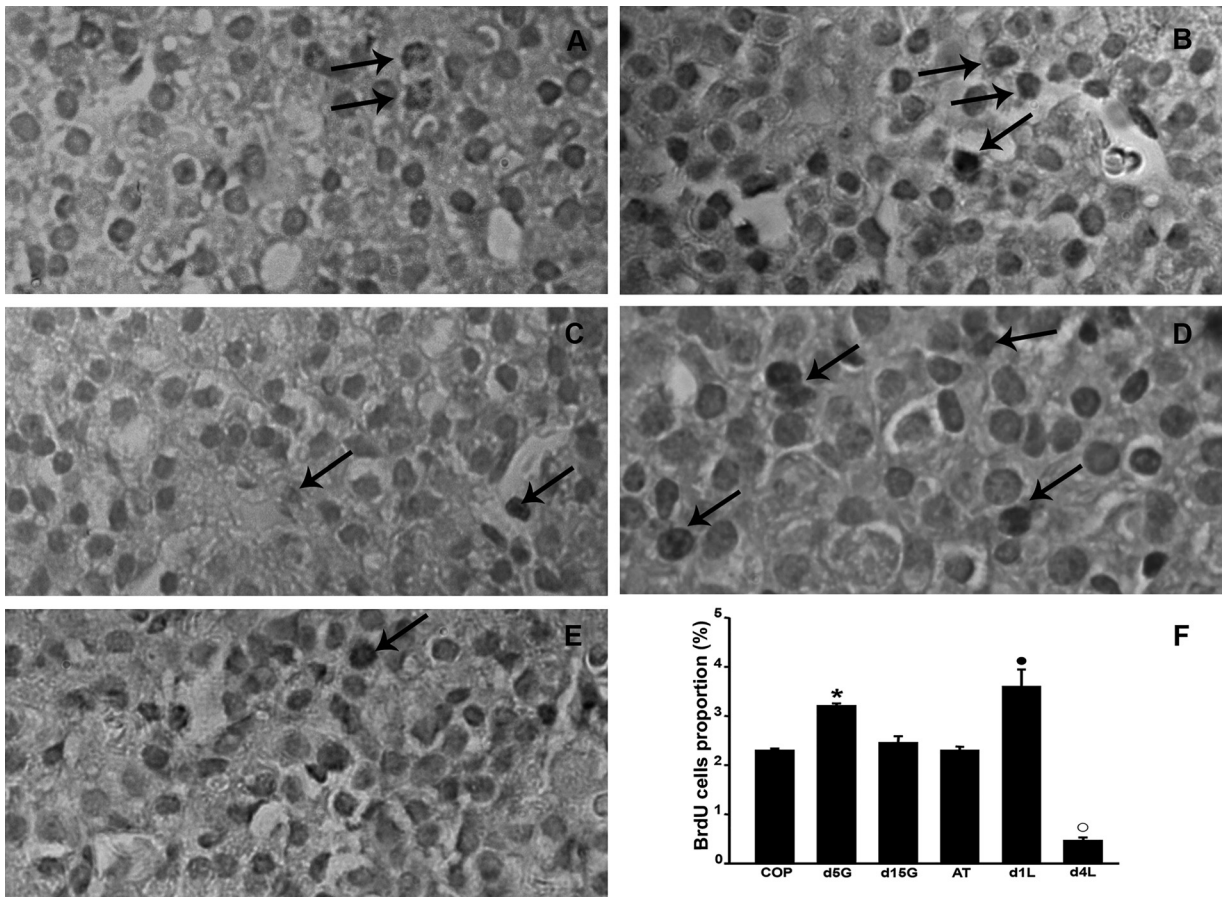

Fig. 8. Cell proliferation in AP cells at gestation and lactation pituitaries. *A–E*: representative light microscope photomicrographs of BrdU-positive cells observed in rats at COP (*A*), d5G (*B*), AT (*C*), d1L (*D*), and d4L (*E*). Arrows highlight selected cells that are positive for BrdU in AP zone. Original magnification, ×400. *F*: The BrdU incorporation in AP increases at d5G (*$P < 0.05$, d5G vs. COP) and at early lactancy (●$P < 0.05$, d1L vs. AT), after which a reduction at d4L is observed (○$P < 0.05$, d4L vs. AT). The BrdU-positive nuclei staining is expressed as the percentage of the total nuclei counted from a total of 5,000 AP cells obtained from randomized samples for each rat. The data are shown as means ± SE of 4 animals/group, with data being evaluated using the ANOVA-Tukey test.

complex regulatory network in the stem fate choice process (4, 43).

A singular subcellular distribution of Sox2 expression was observed at COP and in the middle of the gestation, which was localized more frequently in the nuclear than in the cytoplasmic compartment of MZ cells. The nuclear Sox2 expression has been related to its role as gatekeeper of the pluripotency in embryonic and adult SC (25, 46), whereas the exclusion of Sox2 from the nucleus by nucleocytoplasmic shuttling, for instance, is associated with the inhibition of its activity, thereby allowing pituitary endocrine differentiation (17). In the current study, the mRNA of the progenitor marker Sox9 showed an increase at d15G and active lactancy, whereas its protein levels rose at d1L. These fluctuations detected allowed us to hypothesize that Sox9 could have participated during the activation of the SC/P niche during gestation and lactancy through the expansion of a progenitor cell population, thus acquiring a transitional state before choosing a definitive fate.

The expression of the organ-specific factors Prop1 and Pit-1 may reveal a cell population at a committed precursor stage in the course of differentiation to a specific cell type (54). The mRNA levels of these markers displayed an interesting increase in the MZ and AP in AT and in the early and active lactancy groups. In particular, Prop1 exhibited a noticeable mRNA increment at d1L in the MZ, whereas Pit-1 showed a similar behavior at in AP. We also analyzed the relationship between PROP1/Pit-1 in MZ vs. AP. In MZ, the PROP1 expression was greater than Pit-1 in AT and d1L, whereas this relation was inverted in AP for the same groups. It is possible that the low PROP1 mRNA levels compared with the high Pit-1 levels in AP could have been related to the initiation of differentiation programs similar to those occurring during embryonic development of the hormonal cells (7, 57, 59).

Accumulating evidence has indicated a marked plastic adaptation (21) of the adult pituitary gland occurring mainly in response to hormonal stimulus in the reproductive states (45). Classically, during gestation and lactancy, an increase in the adenohypophysial cell proliferation has been described in humans and rats (1, 24). However, in recent years, it has been shown that the trophic activity under basal conditions as well as in response to hormonal stimuli also occurs in cells that are not hormonally active (36). To date, however, there are no studies that have investigated a differential cell proliferation in the MZ or AP cells during remodeling of the hormonal cells. Therefore, we performed an analysis of the incorporation of BrdU in MZ and AP cells. A remarkable fluctuation in BrdU

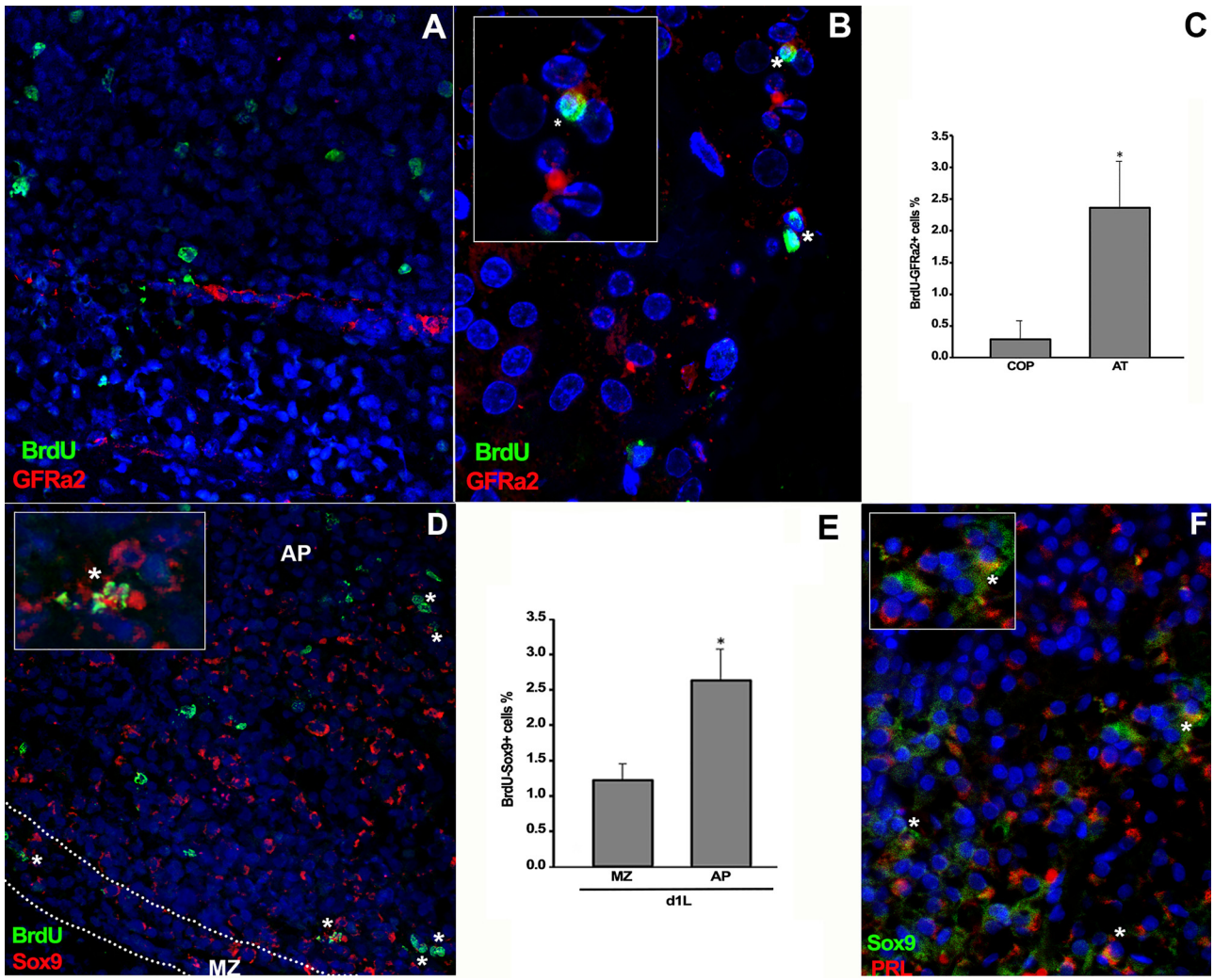

Fig. 9. Double immunofluorescence for BrdU with GFRa2 or Sox9. *A*: coimmunostaining of BrdU and GFRa2 in the MZ of the COP group. Original magnification, ×200. *B*: *BrdU-positive MZ cells showed GFRa2 expression from AT pituitaries. Original magnification, ×600. *C*: an increase in BrdU-GFRa2+ MZ cells occurred in the AT group (*$P < 0.05$, AT vs. COP). BrdU-GFRa2+ cells were expressed as the percentage of total BrdU-positive cells that comprised the 1st and 2nd layers of the MZ obtained from random samples for each rat. Data are shown as means ± SE of 3 animals/group (*t*-test). *D*: *BrdU-Sox9+ cells in the MZ and AP from the d1L pituitary group. Dotted line indicates the limit of the MZ and AP. Original magnification, ×200. *E*: BrdU-Sox9+ cells showed a significant increase in AP in the d1L group (*$P < 0.05$, AP vs. MZ). BrdU-Sox9+ cells were expressed as the percentage of total BrdU-positive cells of the 1st and 2nd layers of MZ and also as a total of 1,000 AP cells obtained from random samples for each rat. Data are shown as means ± SE of 3 animals/group (*t*-test). *F*: *in the AP, some scarce cells coexpressed Sox9 and prolactin (PRL; see *inset*) from the early lactancy pituitaries. Original magnification, ×400.

uptake was observed in MZ cells, showing a significant rise at AT. A different pattern of BrdU uptake was described in AP, with an increase being detected at early lactancy followed by decrease at d4L in the number of BrdU-positive cells in both the MZ and AP zones. Considering the upregulation of SC markers and the increase in cell proliferation in the MZ of the AT group, an expansion of the SC niche in the MZ at term of gestation may be proposed. On analyzing the proliferating cells that expressed the GFRa2 marker in the MZ at term of gestation, a significant increase in BrdU-GFRa2+ cells was observed in the MZ of the AT group, indicating that the pituitary SC that were in a rest condition may have reentered the cell cycle to supply the physiological demands, as reported previously in other adult tissues (52). In a recent report using the lineage-tracing experiment, it was demonstrated that pituitary stem cells are derived from the embryonic Rathke's pouch progenitors and that they continue to proliferate and differentiate to contribute to postnatal pituitary growth (60). For the progenitor marker, we compared the Sox9-proliferating cells in the MZ vs. AP of the d1L group, which described the highest cell proliferation values and observed that the positive cells were significantly greater in the AP. These findings suggest an expansion of the SC pituitary MZ niche at the end of gestation, which may then be mobilized to the AP region as Sox9+ progenitor cells, thus making it possible to differentiate in specific types of endocrine cells at early lactancy.

In conclusion, in the present study, we detected oscillatory patterns in the mRNA and protein levels of the SC/P markers in combination with a remarkable fluctuation in the cell proliferation rate in the MZ during the gestation and lactancy. These data are indicative of a pituitary SC/P niche contribution to supply the demand for new endocrine cells in the reproduc-

tive states studied. A future better understanding of this mechanism may provide significant insights into pituitary SC/P fate choice and also help to shed light on the pituitary plasticity displayed in the physiological environment.

ACKNOWLEDGMENTS

We thank Elena Pereyra for excellent technical assistance. We also thank native speaker Dr. Paul Hobson for revising the English of the manuscript.

GRANTS

This work was supported by the Fondo Nacional de Ciencia y Tecnología (FONCYT), Consejo Nacional de Investigaciones Científicas y Técnicas (CONICET), and Secretaría de Ciencia y Tecnología de la Universidad Nacional de Córdoba (SECyT-UNC).

DISCLOSURES

No conflicts of interest, financial or otherwise, are declared by the authors.

AUTHOR CONTRIBUTIONS

A.M.V. conception and design of research; A.M.V., C.B.G., L.d.V.S., and J.P.N. performed experiments; A.M.V., C.B.G., L.d.V.S., and J.P.N. analyzed data; A.M.V., C.B.G., and L.d.V.S. interpreted results of experiments; A.M.V. and L.d.V.S. prepared figures; A.M.V., J.M., J.P.P., and A.I.T. drafted manuscript; A.M.V., L.d.V.S., J.M., J.P.P., and A.I.T. edited and revised manuscript; A.M.V., C.B.G., L.d.V.S., J.P.N., J.M., J.P.P., and A.I.T. approved final version of manuscript.

REFERENCES

1. **Asa SL, Penz G, Kovacs K, Ezrin C.** Prolactin cells in the human pituitary. A quantitative immunocytochemical analysis. *Arch Pathol Lab Med* 106: 360–363, 1982.
2. **Candolfi M, Zaldivar V, Jaita G, Seilicovich A.** Anterior pituitary cell renewal during the estrous cycle. *Front Horm Res* 35: 9–21, 2006.
3. **Carretero J, Rubio M, Blanco E, Burks DJ, Torres JL, Hernandez E, Bodego P, Riesco JM, Juanes JA, Vazquez R.** Variations in the cellular proliferation of prolactin cells from late pregnancy to lactation in rats. *Ann Anat* 185: 97–101, 2003.
4. **Chang WY, Stanford WL.** Translational control: a new dimension in embryonic stem cell network analysis. *Cell Stem Cell* 2: 410–412, 2008.
5. **Chanson P, Daujat F, Young J, Bellucci A, Kujas M, Doyon D, Schaison G.** Normal pituitary hypertrophy as a frequent cause of pituitary incidentaloma: a follow-up study. *J Clin Endocrinol Metab* 86: 3009–3015, 2001.
6. **Chauvet N, El-Yandouzi T, Mathieu MN, Schlernitzauer A, Galibert E, Lafont C, Le Tissier P, Robinson IC, Mollard P, Coutry N.** Characterization of adherens junction protein expression and localization in pituitary cell networks. *J Endocrinol* 202: 375–387, 2009.
7. **Chen J, Gremeaux L, Fu Q, Liekens D, Van Laere S, Vankelecom H.** Pituitary progenitor cells tracked down by side population dissection. *Stem Cells* 27: 1182–1195, 2009.
8. **Chen J, Hersmus N, Van Duppen V, Caesens P, Denef C, Vankelecom H.** The adult pituitary contains a cell population displaying stem/progenitor cell and early embryonic characteristics. *Endocrinology* 146: 3985–3998, 2005.
9. **Chew LJ, Gallo V.** The Yin and Yang of Sox proteins: Activation and repression in development and disease. *J Neurosci Res* 87: 3277–3287, 2009.
10. **Childs GV.** Development of gonadotropes may involve cyclic transdifferentiation of growth hormone cells. *Arch Physiol Biochem* 110: 42–49, 2002.
11. **D'Amico F, Skarmoutsou E.** Quantifying immunogold labelling in transmission electron microscopy. *J Microsc* 230: 9–15, 2008.
12. **De Paul AL, MJ, Petiti JP, Gutierrez S, Quintar AA, Maldonado CA, Torres AI.** Applications of immunocytochemistry. Immunoelectron microscopy: a reliable tool for the analysis of cellular processes. In: *Biochemistry, Genetics and Molecular Biology*, edited by Dehghani H. Rijeka, Croatia: InTech, 2012, chapt. 4, p. 65–96.
13. **Dinc H, Esen F, Demirci A, Sari A, Resit Gumele H.** Pituitary dimensions and volume measurements in pregnancy and post partum MR assessment. *Acta Radiol* 39: 64–69, 1998.
14. **Elster AD, Sanders TG, Vines FS, Chen MY.** Size and shape of the pituitary gland during pregnancy and post partum: measurement with MR imaging. *Radiology* 181: 531–535, 1991.
15. **Fauquier T, Rizzoti K, Dattani M, Lovell-Badge R, Robinson IC.** SOX2-expressing progenitor cells generate all of the major cell types in the adult mouse pituitary gland. *Proc Natl Acad Sci USA* 105: 2907–2912, 2008.
16. **Fonseca-Pereira D, Arroz-Madeira S, Rodrigues-Campos M, Barbosa IA, Domingues RG, Bento T, Almeida AR, Ribeiro H, Potocnik AJ, Enomoto H, Veiga-Fernandes H.** The neurotrophic factor receptor RET drives haematopoietic stem cell survival and function. *Nature* 514: 98–101, 2014.
17. **Fu Q, Gremeaux L, Luque RM, Liekens D, Chen J, Buch T, Waisman A, Kineman R, Vankelecom H.** The adult pituitary shows stem/progenitor cell activation in response to injury and is capable of regeneration. *Endocrinology* 153: 3224–3235, 2012.
18. **Garcia-Lavandeira M, Diaz-Rodriguez E, Bahar D, Garcia-Rendueles AR, Rodrigues JS, Dieguez C, Alvarez CV.** Pituitary Cell Turnover: From Adult Stem Cell Recruitment through Differentiation to Death. *Neuroendocrinology* 101: 175–192, 2015.
19. **Garcia-Lavandeira M, Quereda V, Flores I, Saez C, Diaz-Rodriguez E, Japon MA, Ryan AK, Blasco MA, Dieguez C, Malumbres M, Alvarez CV.** A GRFa2/Prop1/stem (GPS) cell niche in the pituitary. *PLoS One* 4: e4815, 2009.
20. **Garcia-Lavandeira M, Saez C, Diaz-Rodriguez E, Perez-Romero S, Senra A, Dieguez C, Japon MA, Alvarez CV.** Craniopharyngiomas express embryonic stem cell markers (SOX2, OCT4, KLF4, and SOX9) as pituitary stem cells but do not coexpress RET/GFRA3 receptors. *J Clin Endocrinol Metab* 97: E80–E87, 2012.
21. **Goluboff LG, Ezrin C.** Effect of pregnancy on the somatotroph and the prolactin cell of the human adenohypophysis. *J Clin Endocrinol Metab* 29: 1533–1538, 1969.
22. **Haggi ES, Torres AI, Maldonado CA, Aoki A.** Regression of redundant lactotrophs in rat pituitary gland after cessation of lactation. *J Endocrinol* 111: 367–373, 1986.
23. **Hashi A, Mazawa S, Kato J, Arita J.** Pentobarbital anesthesia during the proestrous afternoon blocks lactotroph proliferation occurring on estrus in female rats. *Endocrinology* 136: 4665–4671, 1995.
24. **Jahn GA, Burdman JA, Deis RP.** Regulation of pituitary DNA synthesis during different reproductive states in the female rat: role of estrogens and prolactin. *Mol Cell Endocrinol* 35: 113–119, 1984.
25. **Kalkan T, Smith A.** Mapping the route from naive pluripotency to lineage specification. *Philos Trans R Soc Lond B Biol Sci* 369: 2014.
26. **Kawaguchi Y.** Sox9 and programming of liver and pancreatic progenitors. *J Clin Invest* 123: 1881–1886, 2013.
27. **Kelberman D, Rizzoti K, Lovell-Badge R, Robinson IC, Dattani MT.** Genetic regulation of pituitary gland development in human and mouse. *Endocr Rev* 30: 790–829, 2009.
28. **Kerr J, Wood W, Ridgway EC.** Basic science and clinical research advances in the pituitary transcription factors: Pit-1 and Prop-1. *Curr Opin Endocrinol Diabetes Obes* 15: 359–363, 2008.
29. **Le Tissier PR, Hodson DJ, Lafont C, Fontanaud P, Schaeffer M, Mollard P.** Anterior pituitary cell networks. *Front Neuroendocrinol* 33: 252–266, 2012.
30. **Lepore DA, Roeszler K, Wagner J, Ross SA, Bauer K, Thomas PQ.** Identification and enrichment of colony-forming cells from the adult murine pituitary. *Exp Cell Res* 308: 166–176, 2005.
31. **Levy A.** Physiological implications of pituitary trophic activity. *J Endocrinol* 174: 147–155, 2002.
32. **Lin H.** Cell biology of stem cells: an enigma of asymmetry and self-renewal. *J Cell Biol* 180: 257–260, 2008.
33. **Mitsiadis TA, Barrandon O, Rochat A, Barrandon Y, De Bari C.** Stem cell niches in mammals. *Exp Cell Res* 313: 3377–3385, 2007.
34. **Mollard P, Hodson DJ, Lafont C, Rizzoti K, Drouin J.** A tridimensional view of pituitary development and function. *Trends Endocrinol Metab* 23: 261–269, 2012.
35. **Niwa H.** How is pluripotency determined and maintained? *Development* 134: 635–646, 2007.
36. **Nolan LA, Levy A.** The trophic effects of oestrogen on male rat anterior pituitary lactotrophs. *J Neuroendocrinol* 21: 457–464, 2009.
37. **Nolan LA, Lunness HR, Lightman SL, Levy A.** The effects of age and spontaneous adenoma formation on trophic activity in the rat pituitary gland: a comparison with trophic activity in the human pituitary and in human pituitary adenomas. *J Neuroendocrinol* 11: 393–401, 1999.

38. **Oishi Y, Okuda M, Takahashi H, Fujii T, Morii S.** Cellular proliferation in the anterior pituitary gland of normal adult rats: influences of sex, estrous cycle, and circadian change. *Anat Rec* 235: 111–120, 1993.
39. **Perez-Castro C, Renner U, Haedo MR, Stalla GK, Arzt E.** Cellular and molecular specificity of pituitary gland physiology. *Physiol Rev* 92: 1–38, 2012.
40. **Porter TE, Wiles CD, Frawley LS.** Evidence for bidirectional interconversion of mammotropes and somatotropes: rapid reversion of acidophilic cell types to pregestational proportions after weaning. *Endocrinology* 129: 1215–1220, 1991.
41. **Rando TA.** Stem cells, ageing and the quest for immortality. *Nature* 441: 1080–1086, 2006.
42. **Rizzoti K, Akiyama H, Lovell-Badge R.** Mobilized adult pituitary stem cells contribute to endocrine regeneration in response to physiological demand. *Cell Stem Cell* 13: 419–432, 2013.
43. **Sampath P, Pritchard DK, Pabon L, Reinecke H, Schwartz SM, Morris DR, Murry CE.** A hierarchical network controls protein translation during murine embryonic stem cell self-renewal and differentiation. *Cell Stem cell* 2: 448–460, 2008.
44. **Sugiyama Y, Ikeshita N, Shibahara H, Yamamoto D, Kawagishi M, Iguchi G, Iida K, Takahashi Y, Kaji H, Chihara K, Okimura Y.** A PROP1-binding factor, AES cloned by yeast two-hybrid assay represses PROP1-induced Pit-1 gene expression. *Mol Cell Endocrinol* 376: 93–98, 2013.
45. **Takahashi S, Okazaki K, Kawashima S.** Mitotic activity of prolactin cells in the pituitary glands of male and female rats of different ages. *Cell Tissue Res* 235: 497–502, 1984.
46. **Tang F, Barbacioru C, Bao S, Lee C, Nordman E, Wang X, Lao K, Surani MA.** Tracing the derivation of embryonic stem cells from the inner cell mass by single-cell RNA-Seq analysis. *Cell Stem Cell* 6: 468–478, 2010.
47. **Toledano Y, Zonis S, Ren SG, Wawrowsky K, Chesnokova V, Melmed S.** Estradiol partially recapitulates murine pituitary cell cycle response to pregnancy. *Endocrinology* 153: 5011–5022, 2012.
48. **Vallier L, Touboul T, Brown S, Cho C, Bilican B, Alexander M, Cedervall J, Chandran S, Ahrlund-Richter L, Weber A, Pedersen RA.** Signaling pathways controlling pluripotency and early cell fate decisions of human induced pluripotent stem cells. *Stem Cells* 27: 2655–2666, 2009.
49. **Vankelecom H.** Non-hormonal cell types in the pituitary candidating for stem cell. *Semin Cell Dev Biol* 18: 559–570, 2007.
50. **Vidal S, Horvath E, Kovacs K, Cohen SM, Lloyd RV, Scheithauer BW.** Transdifferentiation of somatotrophs to thyrotrophs in the pituitary of patients with protracted primary hypothyroidism. *Virchows Arch* 436: 43–51, 2000.
51. **Voog J, Jones DL.** Stem cells and the niche: a dynamic duo. *Cell Stem Cell* 6: 103–115, 2010.
52. **Wabik A, Jones PH.** Switching roles: the functional plasticity of adult tissue stem cells. *EMBO J* 34: 1164–1179, 2015.
53. **Yako H, Kato T, Yoshida S, Higuchi M, Chen M, Kanno N, Ueharu H, Kato Y.** Three-dimensional studies of Prop1-expressing cells in the rat pituitary just before birth. *Cell Tissue Res* 354: 837–847, 2013.
54. **Yako H, Kato T, Yoshida S, Inoue K, Kato Y.** Three-dimensional studies of Prop1-expressing cells in the rat pituitary primordium of Rathke's pouch. *Cell Tissue Res* 346: 339–346, 2011.
55. **Yeo JC, Ng HH.** The transcriptional regulation of pluripotency. *Cell Res* 23: 20–32, 2013.
56. **Yin P, Arita J.** Differential regulation of prolactin release and lactotrope proliferation during pregnancy, lactation and the estrous cycle. *Neuroendocrinology* 72: 72–79, 2000.
57. **Yoshida S, Kato T, Higuchi M, Yako H, Chen M, Kanno N, Ueharu H, Kato Y.** Rapid transition of NESTIN-expressing dividing cells from PROP1-positive to PIT1-positive advances prenatal pituitary development. *J Neuroendocrinol* 25: 779–791, 2013.
58. **Yoshida S, Kato T, Kato Y.** Regulatory System for Stem/Progenitor Cell Niches in the Adult Rodent Pituitary. *Int J Mol Sci* 17: pii: E75, 2016.
59. **Yoshida S, Kato T, Yako H, Susa T, Cai LY, Osuna M, Inoue K, Kato Y.** Significant quantitative and qualitative transition in pituitary stem/progenitor cells occurs during the postnatal development of the rat anterior pituitary. *J Neuroendocrinol* 23: 933–943, 2011.
60. **Zhu X, Tollkuhn J, Taylor H, Rosenfeld MG.** Notch-Dependent Pituitary SOX2(+) Stem Cells Exhibit a Timed Functional Extinction in Regulation of the Postnatal Gland. *Stem Cell Reports* 5: 1196–1209, 2015.